

Enhanced CO<sub>2</sub> Absorption in Organic Solutions of Biobased Ionic Liquids

*Original*

Enhanced CO<sub>2</sub> Absorption in Organic Solutions of Biobased Ionic Liquids / Davarpanah, Elahe; Hernández, Simelys; Latini, Giulio; Pirri, Candido Fabrizio; Bocchini, Sergio. - In: ADVANCED SUSTAINABLE SYSTEMS. - ISSN 2366-7486. - ELETTRONICO. - (2020), p. 1900067. [10.1002/adsu.201900067]

*Availability:*

This version is available at: 11583/2773141 since: 2020-02-06T10:48:12Z

*Publisher:*

Wiley

*Published*

DOI:10.1002/adsu.201900067

*Terms of use:*

This article is made available under terms and conditions as specified in the corresponding bibliographic description in the repository

*Publisher copyright*

(Article begins on next page)

**ADVANCED  
SUSTAINABLE  
SYSTEMS**

Supporting Information

for *Adv. Sustainable Syst.*, DOI: 10.1002/adsu.201900067

Enhanced CO<sub>2</sub> Absorption in Organic Solutions of Biobased  
Ionic Liquids

*Elahe Davarpanah, Simelys Hernández,\* Giulio Latini,  
Candido Fabrizio Pirri, and Sergio Bocchini\**

# SUPPORTING INFORMATION

## Enhanced CO<sub>2</sub> absorption in organic solutions of Bio-based ionic liquids

Elahe Davarpanah,<sup>[a]</sup> Simelys Hernández<sup>[a,b]</sup>,\* Giulio Latini,<sup>[b,c]</sup> Candido Fabrizio Pirri<sup>[b,c]</sup> and Sergio Bocchini<sup>\*[b]</sup>

<sup>a</sup> Catalytic Reaction Engineering for Sustainable Technologies (CREST) Group, Department of Applied Science and Technology (DISAT), Politecnico di Torino, Corso Duca degli Abruzzi, 24, 10129, Turin, Italy.

<sup>b</sup> Centre for Sustainable Future Technologies (CSFT@PoliTo), Istituto Italiano di Tecnologia, Via Livorno, 60, 10144, Turin, Italy.

<sup>c</sup> Department of Applied Science and Technology (DISAT), Politecnico di Torino, Corso Duca degli Abruzzi, 24, 10129, Turin, Italy.

\* E-mail: simelys.hernandez@polito.it, sergio.bocchini@iit.it

### Index

- S1. <sup>1</sup>H-NMR spectra for [Cho][AA] ILs and obtained precipitates**
- S2. Ionic metathesis synthetic path to produce [Cho][AA] ILs**
- S3. ATR-IR spectra of the pure [Cho][AA] ILs**
- S4. Thermo-gravimetric analysis of choline-based AAILs**
- S5. Preliminary absorption studies on [Cho][AA] ILs at various concentration**
- S6. Absorption capacity of all [Cho][AA] ILs solutions during three absorption and desorption cycles**
- S7. Desorption efficiencies of [Cho][AA] ILs solution during three cycles**
- S8. [Cho][AA] ILs solution appearances before and after absorption tests**
- S9. The jacketed bubbling reactor system**

### **S1. <sup>1</sup>H-NMR spectra for [Cho][AA] ILs and obtained precipitates**

The <sup>1</sup>H-NMR analysis was performed with a JEOL JNM-ECZR 600 MHz NMR Spectrometer.

**[Cho][Ala]** (600MHz, DMSO-d<sub>6</sub>) δ: 1.01(s, 3H, CH<sub>3</sub>), 3.10 (s, 9H, CH<sub>3</sub>, CH<sub>3</sub>, CH<sub>3</sub>), 3.28 (t, 1H, CH-N), 3.41(t, 2H, CH<sub>2</sub>), 3.83-3.86 (m, 2H, CH<sub>2</sub>).

**[Cho][Pro]** (600MHz, DMSO-d<sub>6</sub>) δ: 1.38-1.47 (m, 1H, CH<sub>2</sub>), 1.49-1.57 (m, 1H, CH<sub>2</sub>), 1.58-1.66 (m, 1H, CH<sub>2</sub>), 1.72-1.81 (m, 1H, CH<sub>2</sub>), 2.53-2.62 (m, 1H, CH<sub>2</sub>), 2.90-2.97 (m, 1H, CH<sub>2</sub>), 3.00-3.50 (m, 1H, CH), 3.11 (s, 3H, CH<sub>3</sub>, CH<sub>3</sub>, CH<sub>3</sub>), 3.39-3.42 (m, 2H, CH<sub>2</sub>), 3.82-3.86 (m, 2H, CH<sub>2</sub>).

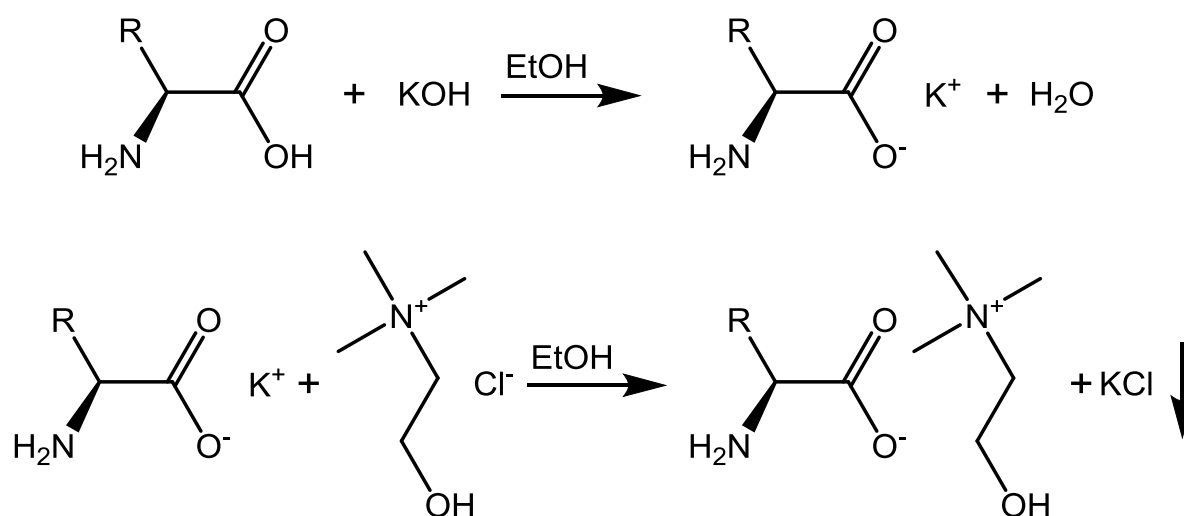
**[Cho][Ser]** (600MHz, DMSO-d<sub>6</sub>) δ: 3.10 (s, 9H, CH<sub>3</sub>, CH<sub>3</sub>, CH<sub>3</sub>), 3.15 (t, 2H, CH<sub>2</sub>), 3.25 (t, 1H, CH-N), 3.40 (t, 2H, CH<sub>2</sub>), 3.82-3.86 (m, 2H, CH<sub>2</sub>).

**[Cho][Gly]** (600MHz, DMSO-d<sub>6</sub>)  $\delta$ : 2.71 (s, 2H, CH<sub>2</sub>), 3.00 (s, 9H, CH<sub>3</sub>, CH<sub>3</sub>, CH<sub>3</sub>), 3.41-3.43 (m, 2H, CH<sub>2</sub>), 3.83-3.86 (m, 2H, CH<sub>2</sub>).

**White precipitate from [Cho][Ala]** (600MHz, D<sub>2</sub>O)  $\delta$ : 1.45 (d, 3H, CH<sub>3</sub>), 3.8 (m, 2H, CH<sub>2</sub>).

**White precipitate from [Cho][Gly]** (600MHz, D<sub>2</sub>O)  $\delta$ : 3.51 (s, 2H, CH<sub>2</sub>).

## S2. Ionic metathesis synthetic path employed to produce [Cho][AA] ILs



## S3. ATR-IR spectra of the pure [Cho][AA] ILs

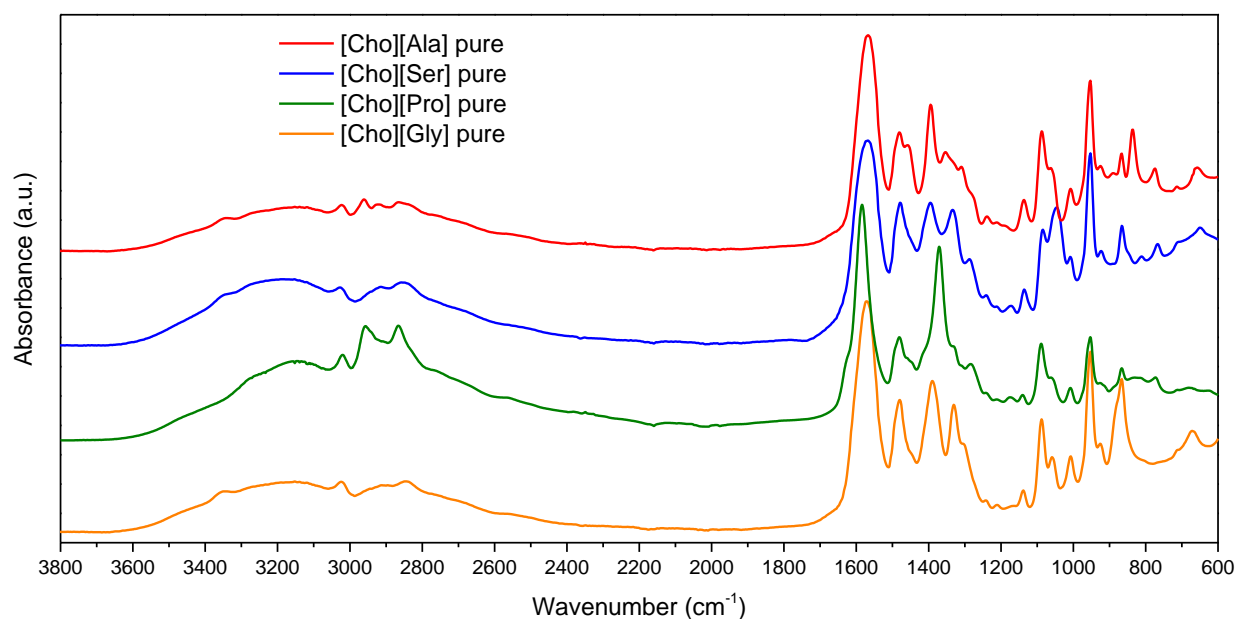


**Figure S1.** ATR-IR spectra of the pure [Cho][AA] ILs.

## Thermo-gravimetric analysis of choline-based AAILs

The TGA analyses were performed on the four [Cho][AA] ILs immediately after rotary evaporation and before the overnight vacuum treatment. All measurements were performed by means of a TG 209 F1 by NETZSCH Thermal Analysis. Approximately 10 mg of sample in alumina pans were heated from 30 to 800 °C (10 °C/min) under synthetic air and pure nitrogen (20 ml/min). In the **Table S1** the degradation temperatures are reported as onset temperature of the different TG curves.

**Table S1:** Degradation temperature determined by  $T_{\text{onset}}$  from TG curves measured under air

Ionic Liquid	$T_{\text{onset}}$ in air (°C)	$T_{\text{onset}}$ in N <sub>2</sub> (°C)
[Cho][Ala]	187	186
[Cho][Pro]	171	171
[Cho][Ser]	183	190
[Cho][Gly]	174	186

(O<sub>2</sub>/N<sub>2</sub> 20:80) and pure nitrogen

## S4. Preliminary absorption studies on [Cho][AA] ILs at various concentration

Preliminary tests were performed on DMSO solution at various concentration of amino acid based ILs. 20 ml of the different solutions were used. During CO<sub>2</sub> absorption the temperature variation was monitored, and the reaction was considered ended once the temperature was constant for 30 seconds (that mean a rate lower than 0.2 °C/min). CO<sub>2</sub> absorption were performed by bubbling 60 ml/min of a gas mixing containing nitrogen/carbon dioxide 4:1. The absorption were performed starting from 25°C and using a falcon where the gas was bubbled. The solution was stirred using a magnetic stirrer. In order to detect any weight loss due to the bubbling process, the ionic liquid solutions were previously tested with pure nitrogen for 30 minutes. No weight variation was found. The CO<sub>2</sub> absorption was evaluated by subtracting the initial weight to the final weight. The results are reported in the **Table S2**, where it is shown that the amount of CO<sub>2</sub> absorbed was the highest for solutions with concentration of 12.5 and 25 wt.% (IL in DMSO). Though in this work [Cho][AA] solutions with concentration of 12.5 wt.% were prepared and tested for dynamic tests with three consecutive absorption-desorption cycles.

**Table S2:** Results of preliminary absorption tests

Absorbent	IL %	DMSO %	CO <sub>2</sub> ads	Ratio CO <sub>2</sub> /IL	ΔT	Time sat
	%wt	%wt	%wt	mol/mol	°C	min
ChoAla	100	0.0	3.8	0.166	6.0	20.0
ChoGly	100	0.0	4.1	0.166	16.0	19.0
ChoGly	87.5	12.5	5.8	0.265	25.9	26.0
ChoGly	75.0	25.0	3.7	0.193	21.5	18.3

ChoGly	50.0	50.0	4.0	0.304	24.5	13.8
ChoGly	25.0	75.0	3.6	0.522	18.0	8.6
ChoGly	12.5	87.5	2.0	0.506	11.7	5.6
DMSO	0.0	100	0.5	-	0.8	6.8

### S5. Absorption capacity of all [Cho][AA] ILs solutions during three absorption and desorption cycles

The absorption capacities of the all ILs solution in DMSO were calculated as moles of CO<sub>2</sub> absorbed for each kg of absorbent and are reported in **Figure S2**. The results show a reduction in the absorption performance of all [Cho][AA] moving from 1<sup>st</sup> cycle to 2<sup>nd</sup> cycle. However, the CO<sub>2</sub> absorption loading remained stable after the 2<sup>nd</sup> cycle for the ILs: [Cho][Pro], [Cho][Ser] and [Cho][Gly]. Instead, for the [Cho][Ala] the CO<sub>2</sub> uptake capacity was also reduced from the 2<sup>nd</sup> to the 3<sup>rd</sup> cycle.

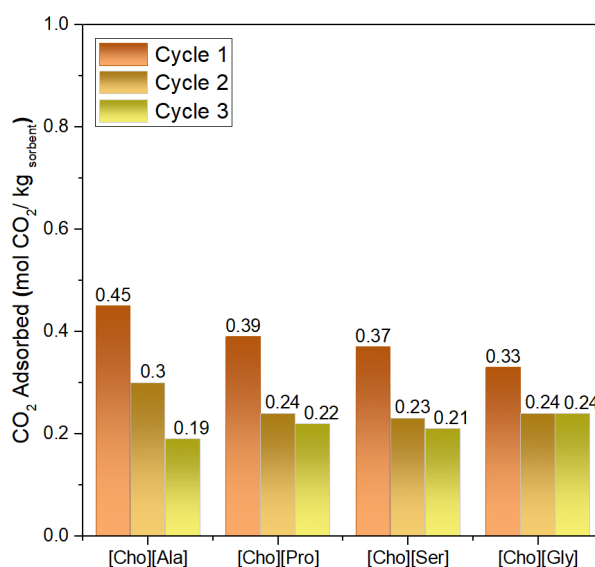


**Figure S2.** Absorption capacities for [Cho][AA]s solutions in DMSO during three cycles

The absorption breakthrough curves during three cycles are shown in **Figure S3**. The breakthrough curves are representing the absorption capacity of each [Cho][AA]s solution during three cycles.

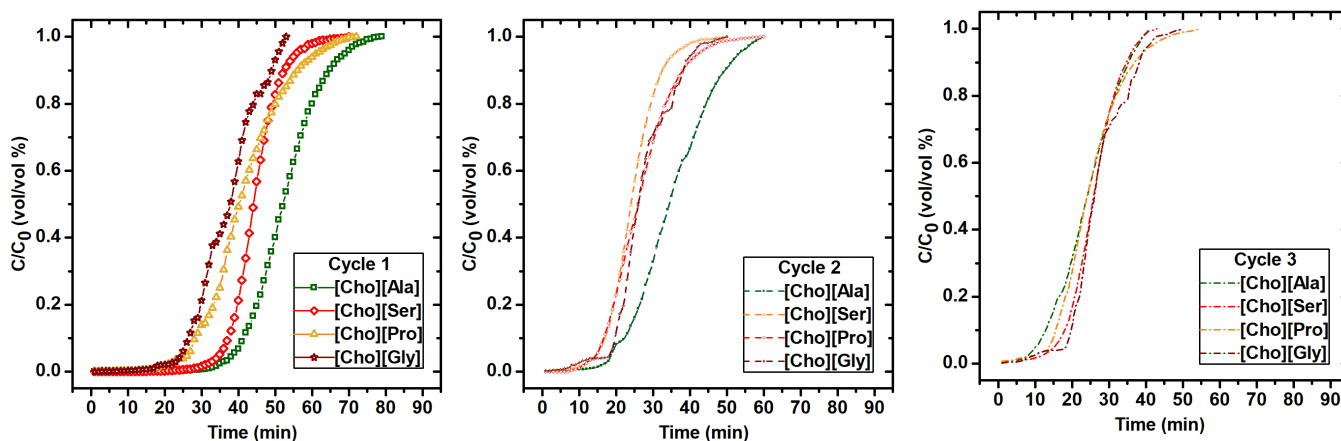


**Figure S3.** Absorption breakthrough curves of all tested ILs in solution with DMSO during three absorption and desorption cycles.

### S6. Desorption efficiencies of [Cho][AA] ILs solution during three cycles

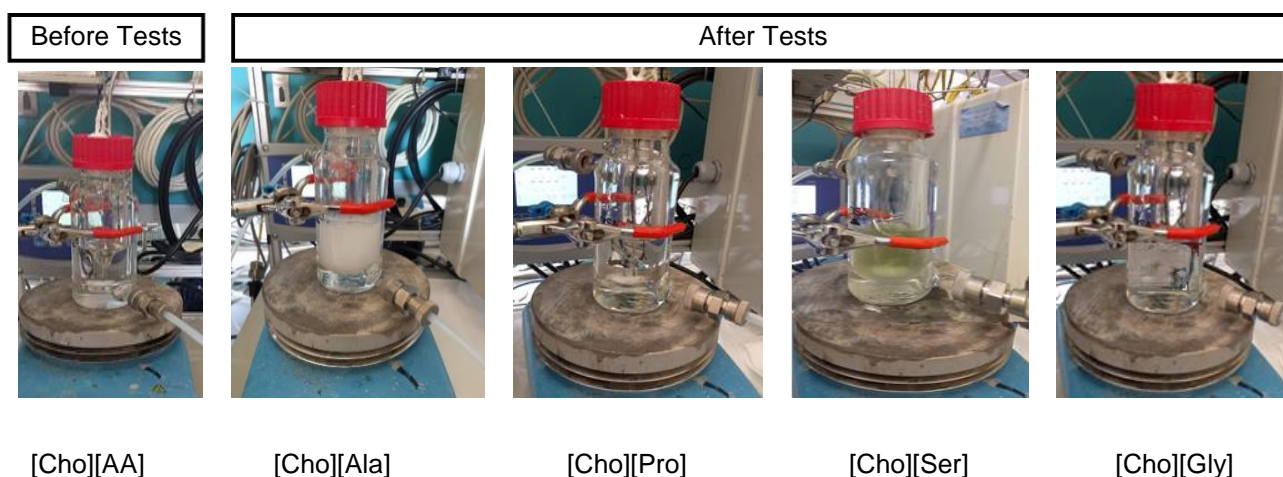
The desorption efficiencies for all [Cho][AA] solutions are calculated by subtracting their absorption amounts and by normalizing it with respect to their initial value during 1<sup>st</sup> and 2<sup>nd</sup> runs, *i.e.* by dividing the calculated desorbed amount by the initial absorption quantity. The results present the desorption efficiency of almost equal to 85% for the [Cho][Ser], [Cho][Pro] and [Cho][Gly] which shows stable absorption capacity. For [Cho][Ala] the absorption behavior showed to be stable in the 3<sup>rd</sup> cycle.

**Table S3:** Desorption efficiency of the ILs after the different absorption-desorption cycles.

Desorption Efficiency (%)		
	Cycle 1	Cycle 2
[Cho][Ala]	36.3	41.9
[Cho][Pro]	39.9	84.3
[Cho][Ser]	35.4	83.2
[Cho][Gly]	30.4	89.2

### S7. [Cho][AA] ILs solution appearances before and after absorption tests

The physical status of the [Cho][AA]s in DMSO solution before and after performing



absorption tests are showed in **Figure S4**. The pictures taken confirm the presence of a white precipitate for all solutions after capturing CO<sub>2</sub>. The nature of such precipitate was analyzed afterward by IR spectroscopy analysis.

**Figure S4.** The state of [Cho][AA]s after absorption test in the laboratory due to precipitation of the solution

### S8. The jacketed bubbling reactor system

The experimental set-up used for the absorption and desorption measurements showed in **Figure S5** consists of a jacketed reactor, a magnetic stirrer, a gas chromatograph, and a circulating thermal bath. The quartz reactor has an internal diameter of 40 mm and a total volume of 125 cm<sup>3</sup>. An external jacket with a thickness of 10 mm is used to maintain the temperature constant due to the exothermic nature of the absorption. The water passed through the jacket using FALC SBF.15 circulating bath with a capacity of 15 L and operating temperature range of -30 - +100 °C. The reactor is sealed with a thick rubber cork stopper (40 mm thickness and 30 mm diameter). The cap has three holes, holding the thermocouple and gas inlet and outlet tubes. The gas is injected into the liquid phase through a stainless-steel tube with an outer diameter (O.D.) of 1/6" placed in the center of the cap. While the outlet gas is exit through a stainless-steel tube of 1/8" O.D.

The operating condition for temperature and pressure were monitored by a K type thermocouple and a pressure transducer connected to the outlet tube. The gas inlet flow rate is controlled by a Bronkhorst® mass flow controller. The system parameters of pressure in the headspace, temperature, flow rate of argon and flowrate of CO<sub>2</sub> are continuously monitored, and data are recorded by using software developed in LABVIEW® platform. The CO<sub>2</sub> volume fraction expressed in ppm in the outlet gas is measured every minute by a micro-Gas Chromatograph (Varian 490-µGM). The GC is equipped with a PoraPLOT Q column of 10 m with a carrier gas of argon and a micro-TCD detector. The column temperature of the GC was kept at 80 °C. The analysis method uses an injection time of 40 ms.

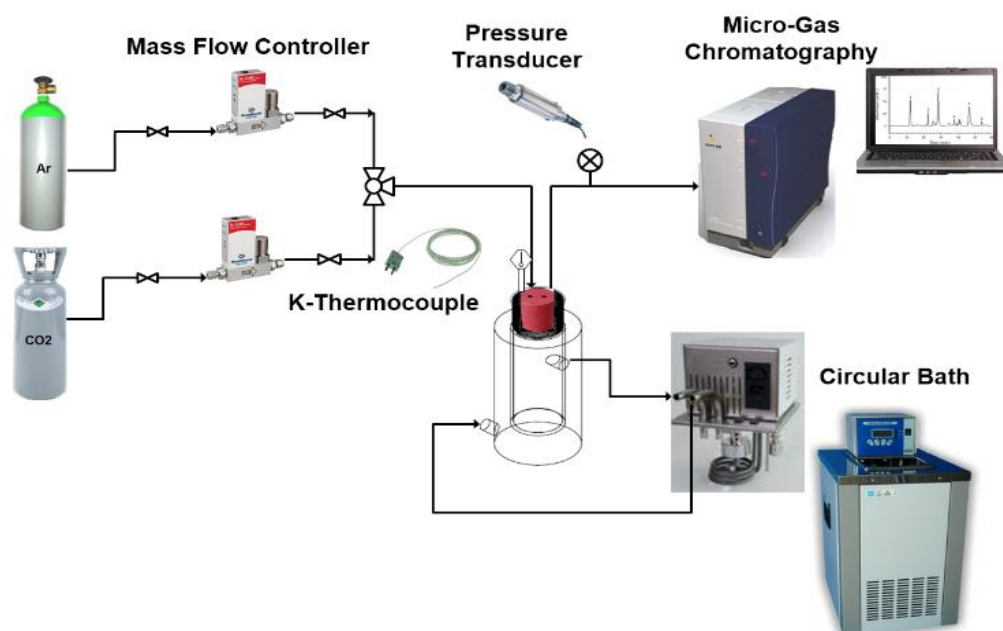


**Figure S5.** Laboratory test-bench for absorption and desorption measurements.